Science Press

ARTICLE

Effects of Zn, Zr, and Dy Addition on Corrosion Resistance and Mechanical Properties of Biomaterial Magnesium Alloy

Shi Huina[1],   He Junguang[1,2,3],   Wen Jiuba[1,2,3],   Li Huan[1],   Tian Peiwu[1]

[1] School of Materials Science and Engineering, Henan University of Science and Technology, Luoyang 471023, China; [2] Collaborative Innovation Center of Nonferrous Metals, Luoyang 471023, China; [3] Provincial and Ministry Co-construction of Collaborative Innovation Center for Non-ferrous Metal New Materials and Advanced Processing Technology, Luoyang 471023, China

Abstract: The effects of micro-alloying treatment on corrosion resistance and mechanical properties of biomaterial magnesium alloy were investigated by optical microscope (OM), scanning electron microscope (SEM), immersion test, electrochemical test, and tensile test. The results show that after successively adding Zn, Zr, and Dy, the grain of magnesium alloys is refined and the second phase is generated and grows up. When Zn, Zr, and Dy are simultaneously added into magnesium alloy, the grain size of alloy is decreased from 1087 μm to 70 μm and the microstructure becomes more uniform. Moreover, the addition of Zn, Zr, and Dy significantly improves the corrosion resistance and mechanical properties of magnesium alloy: the corrosion rate decreases from 2.01 mm/a to 0.92 mm/a; the self-corrosion current density decreases from 4.22 $\mu A/cm^2$ to 2.05 $\mu A/cm^2$; the yield strength, ultimate tensile strength, and elongation increase from 30.5 MPa, 69.5 MPa, and 6% to 84 MPa, 154 MPa, and 8.6%, respectively.

Key words: element addition; magnesium alloys; corrosion resistance; mechanical property

Magnesium alloys can avoid stress shielding effect because their elastic modulus and density are similar to those of human bone. Moreover, magnesium ion is one of the fundamental elements of life activity[1-3]. However, because of the rapid corrosion rate in human body, magnesium alloys can hardly meet the service requirements and may even lead to the accumulation of corrosion products and hydrogen bubbles, which may cause clinical complications for patients[4-6].

To overcome the disadvantages of fast corrosion rate during the service life of magnesium alloys, many studies have been conducted to improve the corrosion resistance, such as micro-alloying, heat treatment, and thermal deformation[7]. Micro-alloying is one of the most basic and important methods of modifying magnesium alloys, which can effectively improve the mechanical properties and corrosion resistance of magnesium. The suitable alloying elements are normally beneficial or at least harmless to humans[8]. Zn and Zr elements have low toxicity to human organs and can promote the growth of human bone cells, which are beneficial for bone healing[9-11]. In addition, they can refine the grains, thus

improving the mechanical properties of magnesium alloys[12-14]. The addition of rare earth elements can significantly improve the mechanical properties and corrosion resistance of magnesium alloys as well[15]. Rare earth elements can eliminate the impurities, increase the electrode potential of magnesium matrix, and form a stable protective film to improve the corrosion resistance of magnesium alloys[16,17]. Among the rare earth elements, Dy element is less toxic than other commonly used rare earth elements, such as Nd, Y, La, and Pr[18,19]. In addition, Dy is soluble in magnesium alloys, which improves the solution strengthening effect, and its electrode potential is higher than that of magnesium, which is beneficial for increasing the electrode potential of the magnesium matrix, thus decreasing the corrosion rate of the alloy[20].

Zhang et al[12] studied Mg-Zn alloys and found that the proper addition of Zn element improves the corrosion resistance and mechanical properties of magnesium alloys. Gandel et al[21] found that the addition of Zr and Sr elements can refine the grains, which is beneficial for the improvement

of the corrosion resistance and mechanical properties of as-cast Mg-Zr-Sr alloys as biodegradable orthopedic implants. Bi et al[22,23] studied the effects of extrusion and heat treatment on the structure, mechanical properties, and corrosion resistance of Mg-1Zn-12Dy alloys and found that the addition of Dy element leads to the formation of long period stacking ordered (LPSO) phase in the alloy and the morphology and distribution of LPSO phase have obvious influence on the mechanical properties and corrosion resistance of the alloy. Yao et al[24] pointed out that the addition of various alloying elements in magnesium alloys contributes to the strengthening of mechanical properties and corrosion resistance of magnesium alloys. However, the high content of the added elements is likely to have adverse effects on human body. For example, excess Zn may cause zinc poisoning. When the content of Zr and Dy is high, Zr and Dy are easy to accumulate in the body and affect human health, especially the organs, such as kidney and liver. Based on the above analysis, this research designed four alloys, namely, Mg, Mg-2Zn, Mg-2Zn-0.5Zr, and Mg-2Zn-0.5Zr-1.5Dy, to analyze the effects of trace Zn, Zr, and Dy addition and the number of alloying elements on the properties of magnesium alloys.

1　Experiment

Different contents of elements Zn, Zr, and Dy were added into magnesium (99.95wt%) to obtain Mg-2Zn, Mg-2Zn-0.5Zr, and Mg-2Zn-0.5Zr-1.5Dy alloys. The alloys were melted in a ZGJL0.01-40-4 type furnace, and the mixed gas of SF_6+CO_2 was used as the protective gas. When the alloys were heated to 740 °C in a graphite crucible and kept at 720 °C for 5 min, the melted alloys were then poured into a preheated steel mold with the size of 160 mm×45 mm×100 mm at 200 °C. Mg (99.95wt%) and Zn (99.99wt%) were added as pure metals, Zr was added as Mg-Zr with 30wt% Zr, and Dy was added as Mg-Dy with 20wt% Dy.

The alloys were machined by cutting-wire into specimens of Φ11.3 mm×8 mm in size. The specimen surface was firstly polished by sandpaper of 800#, 1000#, 1500#, and 2000# and then by the polishing machine. Finally the specimens were washed by pure water and ethanol to observe the micro-structure of the specimen by scanning electron microscope (SEM, JSM-5610LV, JEOL, JAPAN) equipped with an energy dispersive X-ray spectrometer (EDS). The specimen surface was etched and polished by 4vol% nitric acid alcohol solution, and the microstructure was observed by Zeiss optical micro-scope (OM, OLYMPUS PMG3, JAPAN). D8 ADVANCE X-ray diffractometer (XRD) equipped with Cu target Kα rays was used to analyze the phases of alloys. The angle range was set as 15°~85°, and the scanning speed was set as 2°/min.

Specimens with a size of Φ18 mm×5 mm were obtained for the immersion test, and the corrosion was conducted in the simulated body fluid (SBF) solution. The ratio of the SBF volume to the specimen area was 30 mL/cm², the temperature of solution was kept at 37±0.5 °C, the pH value was adjusted to 7.6±0.2, the total immersion duration was 120 h, and SBF solution was replaced every 24 h. The mass of specimens was weighed and recorded. After immersion for 120 h, the specimens were put in chromic acid solution (20wt% CrO_3+ 1wt% $AgNO_3$) and cleaned ultrasonically for 5 min to remove the corrosion products on the surface. After removing the corrosion products, the specimens were weighed and recorded again. The experiment conditions of the hydrogen evolution test were similar, and the hydrogen evolution experiment recorded the amount of released hydrogen every 24 h. The corrosion rate of magnesium alloy could be calculated by Eq.(1), as follows:

$$CR=8.76W\times10^4/A\rho T \tag{1}$$

where CR is the corrosion rate of alloy (mm/a); W is the mass loss after immersion (g); A is the area of specimen (cm²); ρ is the density of alloys (g/cm²); T is the immersion time of alloys (h)[14]. Each type of alloys was tested 3 times.

The specimen size for electrochemical test was Φ11.3 mm× 8 mm. The polarization curve and impedance were obtained by NOVA Autolab electrochemical workstation (AUT84580). The electrochemical test started after the specimen was immersed in SBF solution for 1 h. The potential range of the polarization curve was set as −1.9~−1.2 V, and the scan rate was 0.005 V/s. The impedance frequency range was set as 10^{-1}~10^5 Hz, and the amplitude was 5 mV.

The specimen size for tensile test was set according to the GB6397-86 standard. Shimadzu AG-1250KN material testing machine was used for tensile test at room temperature. The tensile rate was 1 mm/min, and each type of alloys was tested 5 times.

2　Results

2.1　Microstructure

Fig. 1 shows the OM microstructure of Mg and different alloys. The average grain sizes of Mg, Mg-2Zn, Mg-2Zn-0.5Zr, and Mg-2Zn-0.5Zr-1.5Dy alloys are 1087, 181, 144, and 70 μm, respectively. Due to the addition of elements, the grains of alloys are refined. In addition, there are many twins in the crystal grains in as-cast magnesium matrix. With the addition of Zn, the twins disappear and many dendrites appear in the magnesium matrix. Zhang et al[25] found that the second phase is mainly distributed along the dendrite boundary. When Zn and Zr are added, the grains are equiaxed crystal, and the content of the second phase is less. As for Mg-2Zn-0.5Zr-1.5Dy alloy, the grains are equiaxed crystal and the second phase is generated along the grain boundaries.

Fig. 2 shows the SEM microstructure of Mg and different alloys. It can be observed that there are almost no white particles after Zn addition. After Zn and Zr are added, the white particles remain stable. However, the white particles are increased in volume fraction and distributed along the grain boundary after the addition of Zn, Zr, and Dy. EDS analyses show that white particles at point A and B mainly consist of Mg and Zn elements, and those at point C mainly consist of Mg, Zn, and Dy, as shown in Table 1. From Table 1, the second phase of Mg-2Zn and Mg-2Zn-0.5Zr alloys is
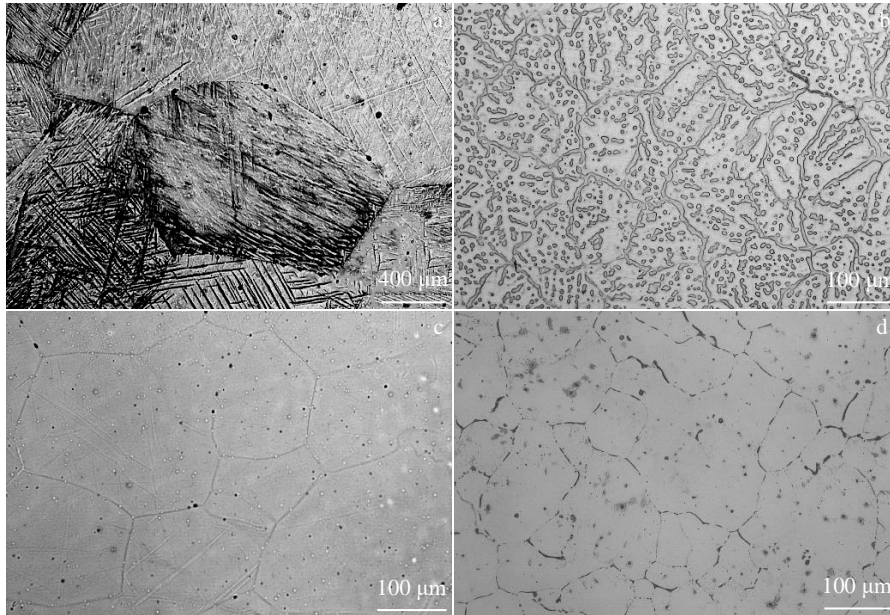
Fig.1   OM microstructures of Mg (a), Mg-2Zn (b), Mg-2Zn-0.5Zr (c), and Mg-2Zn-0.5Zr-1.5Dy (d) alloys
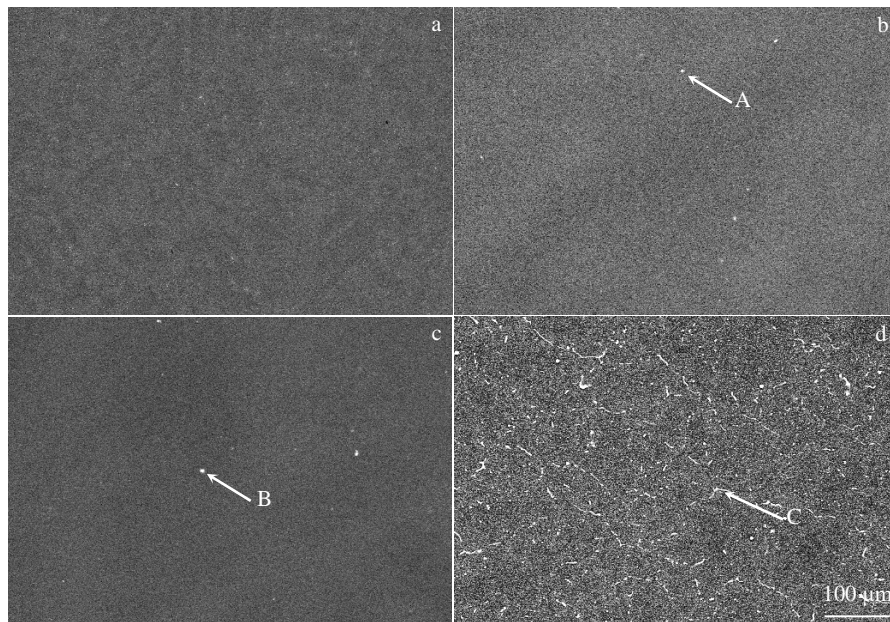
Fig.2   SEM microstructures of Mg (a), Mg-2Zn (b), Mg-2Zn-0.5Zr (c), and Mg-2Zn-0.5Zr-1.5Dy (d) alloys

Table 1   Composition of point A in Fig.2b, point B in Fig.2c, and point C in Fig.2d

Point	Mass fraction/wt%			Atomic fraction/at%		
	Mg	Zn	Dy	Mg	Zn	Dy
A	96.78	3.22	-	98.78	1.22	-
B	96.95	3.05	-	98.84	1.16	-
C	74.21	11.95	13.84	91.93	5.50	2.57

composed of Mg and Zn elements, and the chemical composition is equivalent. The second phase of Mg-2Zn-0.5Zr-1.5Dy is composed of Mg, Zn, and Dy elements.

XRD patterns of different alloys are shown in Fig. 3. Mg-Zn-Dy appears after Dy addition, but the second phase of Mg-Zn cannot be detected because the content is too small. There is little second phase in the alloys, so it can be inferred that some added elements are dissolved into the alloys. Zn and Dy have a good solid solubility in magnesium alloys, which can lead to solid solution strengthening of the alloys and improve the corrosion resistance and mechanical properties of the alloys[26].
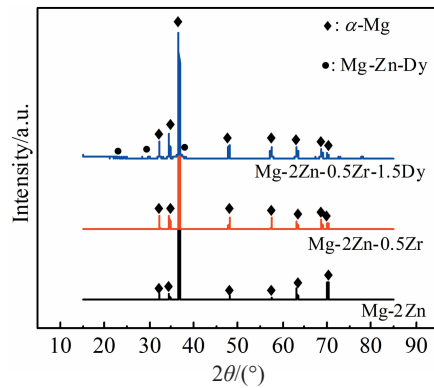
Fig.3　XRD patterns of Mg-2Zn, Mg-2Zn-0.5Zr, and Mg-2Zn-0.5Zr-1.5Dy alloys

2.2　Corrosion resistance

Fig. 4a shows the results of immersion experiment. The corrosion rate of Mg is 2.01 mm/a. With gradually increasing the number of alloying elements, the corrosion rate of alloys is decreased. The corrosion rate of Mg-2Zn-0.5Zr-1.5Dy alloy is the lowest of 0.92 mm/a, and it is reduced by 63.7% compared with that of magnesium matrix. The change trend of corrosion rate result is consistent with that of the hydrogen evolution result, as shown in Fig.4b.

Fig. 4b shows the results of hydrogen evolution of Mg and different alloys. With gradually increasing the number of alloying elements, the volume of released hydrogen is decreased. According to the chemical reaction of $Mg+2H^+=Mg^{2+}+H_2$, it can be seen that the greater the volume of released
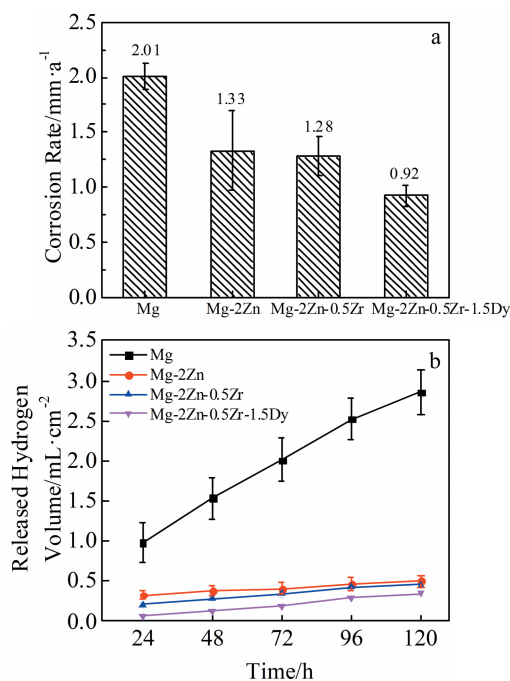
Fig.4　Corrosion rate (a) and average hydrogen evolution rate (b) of Mg and different alloys

hydrogen, the worse the corrosion resistance of alloys. Therefore, the corrosion resistance of the alloys is enhanced after adding alloying elements. The Mg-2Zn-0.5Zr-1.5Dy alloy shows the best corrosion resistance among the investigated alloys, which further proves that the addition of alloying elements is beneficial to improve the corrosion resistance of the magnesium alloys.

Fig. 5 shows the appearances of Mg and different alloys after soaking in SBF solution for 120 h and then removing the corrosion products. With gradually increasing the number of alloying elements, the corrosion situation of alloys is eased, and the surface corrosion morphologies become more and more uniform. The corrosion of Mg specimen is the most serious, showing a large number of corrosion pits. After the addition of Zn element, the corrosion pits on the alloy surface are obviously less. After the addition of Zn and Zr elements, a banded corrosion morphology appears on the alloy surface, and the corrosion pits become shallow. After the addition of Zn, Zr, and Dy elements, the surface corrosion morphology of the alloy is the least serious and uniform, which indicates that the corrosion resistance of the alloy is improved with the addition of Zn, Zr, and Dy elements.

Fig. 6 shows the corrosion morphologies of the specimens after immersion for 120 h. The corrosion morphology of Mg specimen shows mainly big and deep corrosion pits. After adding Zn element, the corrosion pits of the alloy become small and shallow. After adding Zn and Zr elements, the obvious filiform corrosion appears and there are a few small and shallow corrosion pits. After adding Zn, Zr, and Dy elements, the corrosion morphology of the alloy is the least serious, mainly showing the filiform corrosion.

The polarization curves of different alloys after immersion for 1 h are shown in Fig. 7. Based on the polarization curves, the self-corrosion potential (E_{corr}) and self-corrosion current density (I_{corr}) of Mg and alloy specimens can be estimated. As shown in Table 2, I_{corr} of Mg specimen is 4.22 μA/cm². With gradually increasing the number of alloying elements, I_{corr} is gradually decreased. I_{corr} of the Mg-2Zn-0.5Zr-1.5Dy alloy is the minimum of 2.05 μA/cm². E_b is the breakdown potential of the alloy protective film in SBF solution, which can reflect the pitting-corrosion resistance. With gradually increasing the number of alloying elements, E_b of the alloys is increased.

As shown in Fig. 8a~8c, the electrochemical impedance spectroscopy (EIS) diagrams show that the reaction capacity of the alloys in solution is usually based on the magnitude of the arc resistance modulus. The larger the modulus, the greater the reaction resistance and the slower the corrosion rate of anode alloy[27]. According to the impedance curves, the resistance arc of Mg-2Zn-0.5Zr-1.5Dy alloy is the largest, which indicates that Mg-2Zn-0.5Zr-1.5Dy alloy has the best corrosion resistance.

Fig. 8d shows the equivalent circuit obtained from the impedance arc. Since two capacitive arcs appear in the impedance spectrum, there are two time constants in the equivalent circuit. CEP_1 represents the capacitive reactance between the SBF solution and the substrate, and CEP_2
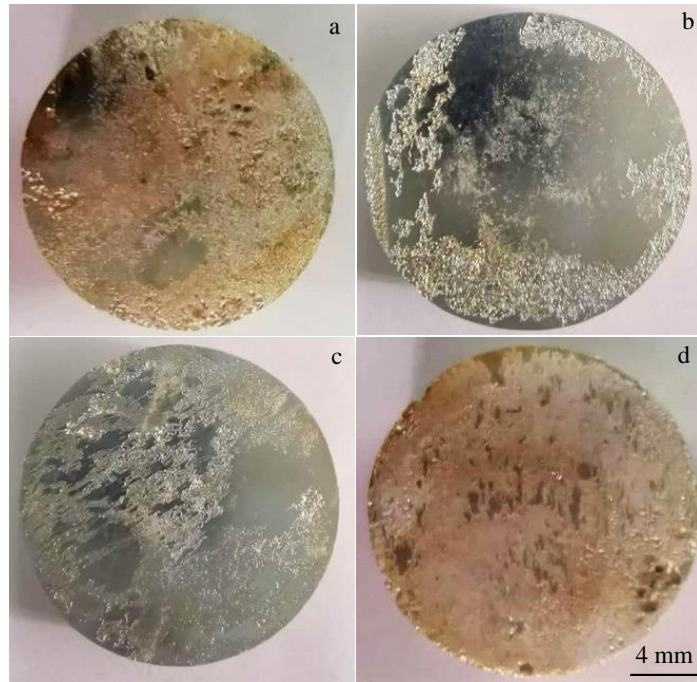
Fig.5　Appearances of Mg (a) and different alloys after immersion for 120 h: (b) Mg-2Zn, (c) Mg-2Zn-0.5Zr, and (d) Mg-2Zn-0.5Zr-1.5Dy
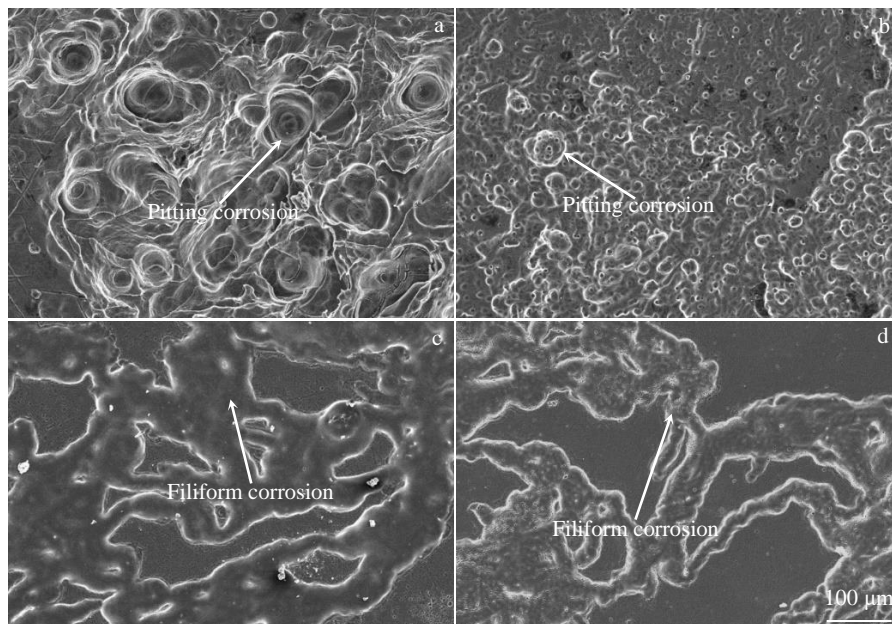
Fig.6　Corrosion morphologies of Mg (a) and different alloys after immersion for 120 h: (b) Mg-2Zn, (c) Mg-2Zn-0.5Zr, and (d) Mg-2Zn-0.5Zr-1.5Dy

represents the double-layer capacitive reactance between the substrate and the solution. R_s, R_1, and R_2 denote the solution resistance, corrosion product layer resistance, and Faraday resistance, respectively. Table 3 shows the soft fitting results of the corresponding equivalent circuits of Mg and different alloy specimens. It can be seen from the results that when Zn, Zr, and Dy elements are added, the sum of R_1 and R_2 is the largest, indicating that the exchange of electronegative ions is difficult and the corrosion rate of the alloy is the lowest.

2.3　Mechanical properties

Fig. 9 shows the tensile test results of Mg and different alloys. The yield strength (YS), ultimate tensile strength (UTS), and elongation (EL) of Mg specimen are 30.5 MPa, 69.5 MPa, and 6%, respectively. With gradually increasing the
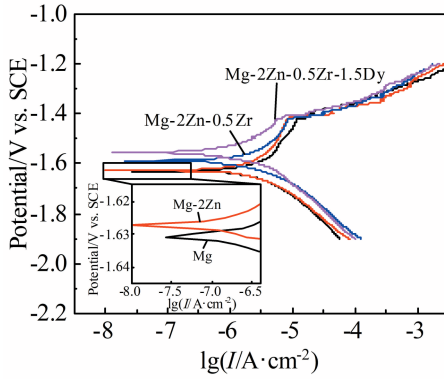
Fig.7　Polarization curves of Mg and different alloys after immersion in SBF solution for 1 h

Table 2　Related experiment results from polarization curves

Specimen	E_{corr}/V	I_{corr}/μA·cm^{-2}	E_b/V
Mg	-1.64	4.22	-1.44
Mg-2Zn	-1.63	3.16	-1.43
Mg-2Zn-0.5Zr	-1.59	2.37	-1.43
Mg-2Zn-0.5Zr-1.5Dy	-1.55	2.05	-1.40

number of alloying elements, the comprehensive mechanical properties of magnesium alloys are gradually optimized. Mg-2Zn-0.5Zr-1.5Dy alloy has the best comprehensive mechanical properties and its YS, UTS, and EL are 84 MPa, 154 MPa, and 8.6%, which are 83%, 121.6%, and 43.3%

higher than those of Mg specimen, respectively.

3　Discussion

The pitting corrosion occurs due to the potential difference between the particles in the alloy and the magnesium matrix, which alleviates the corrosion of magnesium in SBF solution. The greater the potential difference, the faster the corrosion rate. When the magnesium matrix around the particles is dissolved in SBF solution, the particles fall off to form pits. The pitting corrosion can be formed deeply in the alloy, so it has a great influence on the mechanical properties of the alloy. Filiform corrosion is formed because the protective film can be easily formed on the surface of magnesium alloys. The surface with initial protective film cannot be easily corroded in SBF solution, but the surface without protection can be easily corroded. Therefore, the corrosion occurs along the edge of the film layer and a new film layer can be continuously formed after corrosion, which can slow the corrosion rate of alloys[24].

Magnesium alloy contains impurity particles which may easily cause a potential difference between impurity particles and the magnesium matrix, and accelerate the corrosion of the magnesium matrix around the impurity particles[28]. After the impurity particles fall off, the corrosion pits are formed. With the addition of Zn element, the Mg-Zn phase appears in the alloy and then forms a potential difference between the magnesium matrix and the surrounding Mg-Zn phase. When the alloys are immersed in SBF solution, the magnesium matrix can easily lose electrons and be corroded. After the second phase falls off, the corrosion pits appear[12]. Yang et al[29] found that the addition of Zr element can reduce the
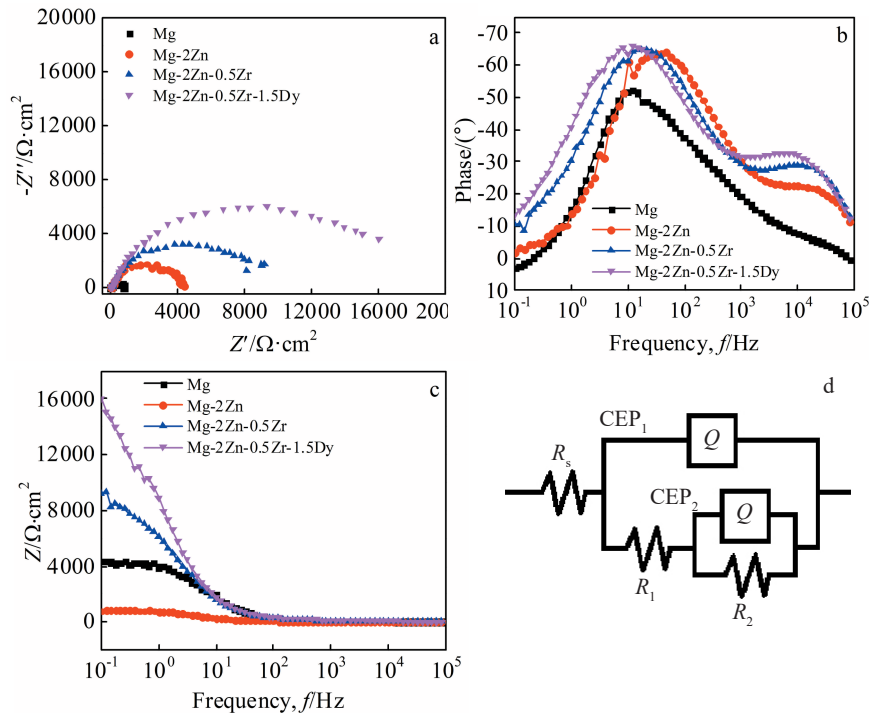
Fig.8　EIS diagrams (a~c) and equivalent EIS circuit (d) of Mg and different alloys: (a) Nyquist diagram, (b) Bode diagram of phase-frequency, and (c) Bode diagram of *Z*-frequency

Table 3 Soft fitting results of EIS circuit of Mg and different alloy specimens in SBF solution

Specimen	R_s/Ω	$CEP_1/\times10^{-5}$ F·cm^2	n	$R_1/\Omega\cdot$cm^2	$CEP_2/$F·cm^2	$R_2/\Omega\cdot$cm^2
Mg	28.95	1.42	0.688	110.7	3.96×10^{-4}	4392
Mg-2Zn	27.52	7.478	0.758	104.8	2.65×10^{-5}	7233
Mg-2Zn-0.5Zr	21.59	2.306	0.630	181.5	4.50×10^{-6}	9788
Mg-2Zn-0.5Zr-1.5Dy	2573.00	1.886	0.640	309.2	4.27×10^{-6}	18 140
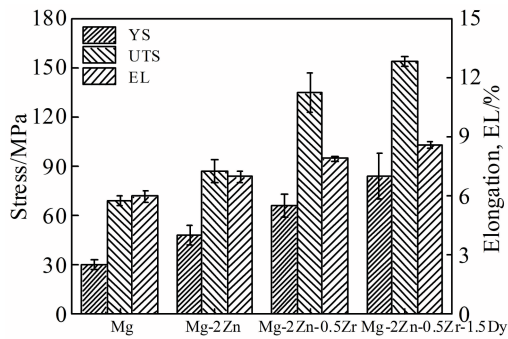
Fig.9 Mechanical properties of Mg and different alloys

influence of Fe and other impurity elements on the corrosion resistance of magnesium alloys, thereby improving the corrosion resistance of the alloys. With the addition of Zn and Zr elements, the impurity elements in the alloy are purified and a protective film is formed due to the second phase particles. Therefore, the surface of the Mg-2Zn-0.5Zr alloy is pitted, and filiform corrosion occurs at the outside of alloys. As for Mg-2Zn-0.5Zr-1.5Dy alloy, there is a large amount of Mg-Zn-Dy phase distributed along the grain boundaries, which leads to the formation of a large area of protective film. So the alloy presents filiform corrosion in SBF solution. Zong et al[30] also believed that the fine and continuous second phase (Fig. 2d) is beneficial to slow down the corrosion rate of magnesium alloys, and magnesium alloys with pitting corrosion are not suitable for implantation material, such as cardiovascular stents, in human body.

Zr element can purify the impurity elements in magnesium, thereby improving the corrosion resistance of alloys. The standard electrode potential of Zn (-0.76 V) and Dy (-2.35 V) is higher than that of the Mg matrix (-2.37 V) [31,32]. Zn and Dy can dissolve in Mg matrix, then improve the electrode potentials of Mg alloys, reduce the potential difference between Mg matrix and the second phases, and finally slow down the corrosion rate of alloys in SBF solution. Therefore, with the addition of alloying elements, the corrosion resistance of the alloy is gradually increased, and the corrosion rate of the alloys is gradually decreased. Mg-2Zn-0.5Zr-1.5Dy alloy has the lowest corrosion rate and its corrosion morphology shows mainly filiform corrosion. So Mg-2Zn-0.5Zr-1.5Dy alloy is a more suitable implant material for human body.

The characteristic of I_{corr} and E_b from the electrochemical test system can reflect the corrosion rate of alloys. The lower the I_{corr}, the better the corrosion resistance of the alloy[33,34]. The higher the E_b, the stronger the pitting-corrosion resistance[35]. According to the polarization curves in Fig. 7, I_{corr} and E_b can be calculated (Table 2). It can be seen that with the addition of alloying elements, I_{corr} is decreased and E_b is increased. The Mg-2Zn-0.5Zr-1.5Dy alloy has the lowest I_{corr} of 2.05 µA/cm^2 and the highest E_b of -1.40 V. Therefore, it can be concluded that the corrosion resistance of the Mg-2Zn-0.5Zr-1.5Dy alloy is the best and the addition of Zn, Zr, and Dy elements can improve the pitting-corrosion resistance of the magnesium alloys.

The UTS is increased from 69.5 MPa to 154 MPa, and the YS is increased from 30.5 MPa to 84 MPa because of the addition of Zn, Zr, and Dy elements. During the tensile deformation of alloys, lattice distortion occurs at the grain boundaries. Slippage needs to overcome the hindrance of the grain boundaries[4]. The finer the alloy grains, the greater the resistance of the grain boundaries to the slippage and the greater the force required for slippage.

Besides, the pinning of the second phase particles can also hinder the slippage. Due to the addition of alloying elements, the grain is refined and the second phase are generated, thereby improving the overall mechanical properties of the alloys. In addition to the strengthening effects of the intermetallic phase, the addition of Dy may also contribute to the solid solution strengthening of the Mg matrix[36]. The large difference in the atomic radius between Dy (0.1774 nm) and Mg (0.1602 nm) may lead to the significant lattice distortion. Therefore, the tensile strength is increased by adding Dy element. The small grain size increases or activates the grain boundary sliding and torsion of the basic slip system and angular slip system, shortens the distance of dislocation movement, and greatly improves the plasticity[28]. Chen et al[37] believed that the refined grains and the redistribution of the second phase can also affect the mechanical properties of the alloys. According to Hall-Patch theory, the dislocations can be propagated from one type of grains to another one through the grain boundary. The increase of grain boundaries in number caused by grain refinement may hinder the dislocation propagation, resulting in an increase in the strength of the alloy with fine grains. In addition, it is also found that the grain refinement of magnesium alloys can increase or activate the sliding of the matrix and the pyramid, promote the sliding and rotation of the grain boundaries, and shorten the movement distance of dislocations, thereby greatly improving the plastic deformation ability of magnesium alloys.

4 Conclusions

1) The addition of Zn, Zr, and Dy elements can refine the grain size, reduce the self-corrosion current density, and enhance the corrosion resistance of magnesium alloys.

2) As for magnesium-based alloys, the strengthening effect of Mg-Zn and Mg-Zn-Dy phases and the solid solution strengthening effect caused by Dy element can lead to the enhancement of yield strength of alloys. Mg-2Zn-0.5Zr-1.5Dy alloy shows the highest yield strength.

3) With the addition of Zn, Zr, and Dy elements, the corrosion resistance and mechanical properties of alloys are greatly improved.

References

1   Zhang Jia, Zong Yang, Yuan Guangyin *et al. The Chinese Journal of Nonferrous Metals*[J], 2010, 20(10): 1989 (in Chinese)
2   Moussa M E, Mohamed H I, Waly M A *et al. Journal of Alloys and Compounds* [J], 2019, 792: 1239
3   Chen Yang, Dou Jiehe, Yu Huijun *et al. Journal of Dental Biomaterials*[J], 2019, 33(10): 1348
4   Banerjee P C, Saadi S A, Choudhary L *et al. Materials*[J], 2019, 12(1): 136
5   Nurettin S, Zafer E, Said M K *et al. Journal of Magnesium and Alloys*[J], 2018, 6(1): 23
6   Li H, Wen J B, He J G *et al. Advanced Engineering Materials*[J], 2020, 22(4): 1 901 360
7   Xu D Z, He J G, Wen J B *et al. Mater Res Exp*[J], 2019, 6(12): 125 411
8   Chen J X, Tan L L, Yu X M *et al. J Mech Behav Biomed*[J], 2018, 87: 68
9   Li Y C, Wen C E, Mushahary D *et al. Acta Biomaterialia*[J], 2012, 8(8): 3177
10 Cai C, Song R, Wang L *et al. Surf Coat Technol*[J], 2018, 342: 57
11 Qin Hui, Zhao Yaochao, An Zhiquan *et al. Biomaterials*[J], 2015, 53: 211
12 Zhang Shaoxiang, Zhang Xiaonong, Zhao Changli *et al. Acta Biomaterialia*[J], 2010, 6(2): 626
13 Peng G S, Wang Y, Fan Z. *Metall Mater Trans A*[J], 2018, 49(6): 2182
14 Zhang Jinyang, Jia Peng, Xu Shumin *et al. Mater Res Exp*[J], 2018, 5(1): 16 506
15 Li Huan, Wen Jiuba, He Junguang *et al. Transactions of Materials and Heat Treatment*[J], 2019, 40(7): 6 (in Chinese)
16 Munir K, Lin J X, Wen C E *et al. Acta Biomaterialia*[J], 2020, 102: 493
17 Zhao Xu, Shi Lingling, Xu Jian. *J Mater Sci Technol*[J], 2013, 29(9): 781
18 Yang L, Hort N, Laipple D *et al. Acta Biomaterialia*[J], 2013, 9(10): 8475
19 Ding Yunfei, Lin Jixing, Wen Cuie *et al. J Biomed Mater Res Part B*[J], 2018, 106(6): 2425
20 Ding Y F, Wen C, Hodgson P *et al. Journal of Materials Chemistry B*[J], 2014, 2(14): 1912
21 Gandel D S, Easton M A, Gibson M A *et al. Corrosion Science* [J], 2014, 81: 27
22 Bi Guangli, Jiang Jing, Zhang Fan *et al. J Rare Earths*[J], 2016, 34(9): 931
23 Bi G L, Li Y D, Huang X F *et al. Mater Sci Eng A*[J], 2015, 622: 52
24 Yao Huai, Wen Jiuba, Xiong Yi *et al. Rare Metal Materials and Engineering*[J], 2019, 48(6): 1982 (in Chinese)
25 Zhang B P, Wang Y, Geng L *et al. Mat Sci Eng A*[J], 2012, 539: 56
26 Long T, Zhang X H, Huang Q L *et al. Virtual and Physical Prototyping* [J], 2018, 13(2): 71
27 Zhang Xiaobo, Yuan Guangyin, Wang Zhangzhong. *The Chinese Journal of Nonferrous Metals*[J], 2013, 23(4): 905 (in Chinese)
28 Esmaily M, Svensson J E, Fajardo S *et al. Progress in Materials Science*[J], 2017, 89: 92
29 Yang Chubin, Zhang Zhen, Jiang Xinyi *et al. Foundry*[J], 2019, 68(7): 684 (in Chinese)
30 Zong Y, Yuan G Y, Zhang X B *et al. Mater Sci and Eng B*[J], 2012, 177(5): 395
31 Bordbar-Khiabani A, Yarmand B, Mozafari M. *Emerging Materials Research*[J] 2019, 8(3): 305
32 Yang L, Ma L G, Huang Y D *et al. Materials Science & Engineering C*[J], 2017, 75: 1351
33 Li T, Zhang H L, He Y *et al. Journal of Materials Science and Technology*[J], 2015, 31(7): 744
34 Chen Junxiu, Tan Lili, Yang Ke *et al. Bioactive Materials*[J], 2017, 2(1): 19
35 Lin D J, Hung F Y, Liu H J *et al. Advanced Engineering Materials*[J], 2017, 19(11): 1 700 159
36 Yang L, Huang Y D, Feyerabend F *et al. J Mech Behav Biomed* [J], 2012, 13: 36
37 Chen L X, Sheng Y Y, Wang X J *et al. Materials*[J], 2018, 11(4): 55

添加 **Zn**、**Zr**、**Dy** 元素对生物镁合金耐蚀性能和力学性能的影响

师慧娜[1]，贺俊光[1,2,3]，文九巴[1,2,3]，李　欢[1]，田培梧[1]
(1. 河南科技大学 材料科学与工程学院，河南 洛阳 471023)
(2. 有色金属协同创新中心，河南 洛阳 471023)
(3. 有色金属新材料与先进加工技术省部共建协同创新中心，河南 洛阳 471023)

摘　要：通过光学显微镜（OM）、扫描电子显微镜（SEM）、浸泡实验、电化学测试和拉伸试验研究了微合金化处理对生物材料镁合金的耐蚀性能和力学性能的影响。结果表明，随着Zn、Zr、Dy元素的添加，镁合金的晶粒得以细化，合金内部第二相生成并长大。将元素Zn、Zr、Dy同时添加到镁合金中时，合金的晶粒尺寸从1087 μm减小到70 μm，显微组织也变得更均匀。此外，添加Zn、Zr、Dy元素可显著改善镁合金的耐腐蚀性和力学性能。根据浸泡实验可知，添加不同元素后，合金的腐蚀速率从2.01 mm/a降低至0.92 mm/a；自腐蚀电流密度从4.22 μA/cm² 降低至2.05 μA/cm²；屈服强度、极限抗拉伸强度和伸长率从30.5 MPa、69.5 MPa和6%增加到84 MPa、154 MPa和8.6%。
关键词：元素添加；镁合金；耐蚀性能；力学性能

作者简介：师慧娜，女，1995年生，硕士生，河南科技大学材料科学与工程学院，河南 洛阳 471023，E-mail：shn1995@126.com